Internet of Things-enabled Hospital Wards – Ultra Wideband Doctor-Patient Radio Channels

Philip A. Catherwood and James McLaughlin

Abstract—**As Ultra Wideband technology re-emerges as a high-data rate solution for the Internet of Things, we consider the application of the technology to medical environments. We present supporting empirical and statistical modelling investigations into body-to-body Ultra wideband Internet of Things links for a bed-bound patient and a roaming clinician conducting routine medical rounds. Of interest is the statistical parameters that indicate link reliability as well as inter-symbol interference probability for a patient in two most likely postures combined with two likely locations of radio antenna for the roaming clinician (antennas in a handheld tablet and on the clinician's waist) to create deployment data for futuristic Internet of Things-enabled hospital environments. The RSSI, mean excess delay and the RMS delay spread results indicate that the use of UWB as an enabling IoT technology in such environments would be generally robust for patients in varying postures, as well as nodes positioned either on the clinician or realized in handheld formats. The spread of received power is best mathematically modelled by the Lognormal distribution for each combination of patient position and clinician antenna location. Both the t_{mean} and the t_{RMS} for each combination can be generally best modelled by the Weibull distribution.**

***Index Terms*— Body-to-body, Hospital, Internet of Things, Propagation, Wearable, Ultrawideband.**

I. Introduction

Ultrawideband (UWB) at one time seemed to have lost its momentum and promise of impact after multiple attempts to agree on standardization ended in deadlock between warring commercial factions [1], however it has been recently rejuvenated through new applications for the Internet of Things [2, 3].

Ongoing UWB IoT antenna development research work is evident within the UWB community [4].The original UWB standardization focused around the IEEE 802.15.3a standard, however the new class of UWB applicable to Internet of Things is aligned with the IEEE 802.15.4a standard which includes the addition of a new PHY layer. [2]. Advances in hospital monitors have produced self-contained portable devices that implement wireless data transfer, diagnostic algorithms [5] as well as manifold benefits over the bedside machines they are replacing [6]. As novel supporting technologies emerge however there are new opportunities to accomplish advances which until recently were unattainable. This is guided by [7] who advocate "Clinically led improvement, enabled by new technology".

Manuscript received November 07, 2017. Philip A. Catherwood is with the Ulster University, UK (e-mail: p.catherwood@ulster.ac.uk).
James McLaughlin is with Ulster University, UK (e-mail: jad.mclaughlin@ulster.ac.uk).

Correct implementation of health service digital technology could result in £10 billion efficiency savings in England by 2020 [8]. Additionally, IoT is set to have a disruptive impact across industry and society, with [9] forecasting 25 billion IoT connected devices by 2020. Key drivers of our work include the global ageing population [10], an increase in chronic conditions [11], current international health economics, the emergence of advanced enabling technologies, and increasing need for earlier diagnosis and predictive analysis [12]. Emerging IoT solutions will offer autonomous low-power data transfer and control which supports the trend towards increasing implementation of technology to reduce distractions and workload on doctors, nurses, and support staff [13,14]. Future hospital solutions are likely to follow commercial partners of adopting ubiquitous computing strategies to deliver intelligent diagnostics [15].

An amount of body-to-body work has been presented in literature including static frequency domain measurements conducted in an anechoic chamber [16], laboratory/office and corridor [17], investigations into receive power levels at disaster sites [18], in a laboratory at 2.45 GHz [19], in a University at 3.8 GHz [20], etc., none of which are suitably applicable to hospital environments which have unique properties. We present futuristic Internet of Medical links between a patient and a roaming clinician while conducting ward rounds in contemporary hospital environments. It examines patient posture effects on the UWB link as well as clinician radio location strategies. To date there is no suitably identical work in the literature and the presented results help to scientifically quantify the radio environment into which medical IoT devices may be deployed.

II. Experimental Arrangements

A. Measurement System

The UWB system had the transmitter on the patient and the receiver on the mobile clinician. The transmitter was a battery-powered UWB PulsON 210 source with an UWB Fractus chip antenna connected (EB-UM-FR05-S1-P-0-107). This transmit antenna, which was worn on the waist of a roaming clinician for one test and embedded into a handheld tablet device for another, was a vertically-polarized antenna with an omni-directional radiation pattern and an average gain of 1.55 dBi. The antenna PCB measured 20.0 x 36.5 x 1.6 mm with the fractal chip antenna measuring 10 x 10 x 0.8 mm. This antenna had a return loss of typically –11 dB, VSWR of 1.45:1, and boresight gain in the region of 3.5 dBi for an isolated antenna.

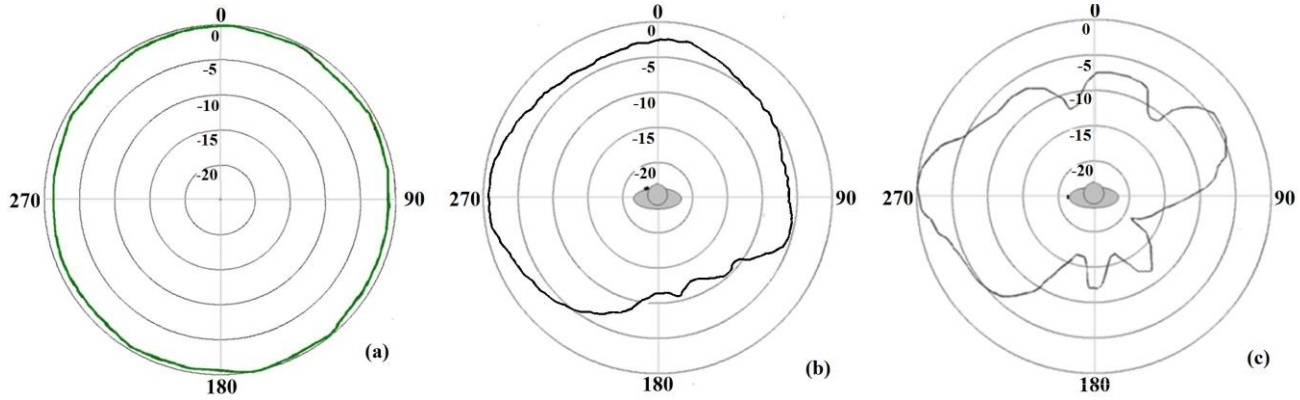

Fig. 1. Transmit antenna wideband azimuthal radiation pattern.
(a) Isolated antenna (b) Waist-worn antenna (c) Handheld device

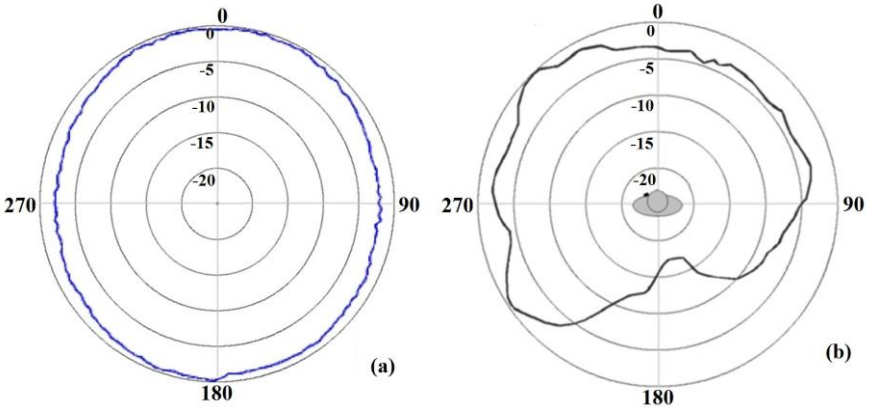

Fig. 2. Receive antenna wideband azimuthal radiation pattern.
(a) Isolated antenna (b) Chest-mounted antenna

The receiver was a corresponding UWB PulsON 210 radio with a PulsON UWB antenna. This receive antenna (which was worn on the chest by the patient) was a vertically-polarized electrically small UWB bottom-fed planar elliptical dipole [21]. Return loss was typically –15 dB, VSWR of about 1.5:1, and boresight gain was in the region of 2 dBi for an isolated antenna. The planar elliptical dipole element is 0.14λ at its lowest frequency of operation [22]. The antennas were (factory) optimized for use with UWB impulses operating in the 3 GHz to 6 GHz and incorporate a balun transformer to improve matching and reduce unwanted cable currents [23]. The balun transformer (at the base of the antenna) facilitates the connection between the balanced dipole structure and the unbalanced coaxial cable [23]; this helps to avoid spurious distorting currents on the cable's sheath. Fig. 1 and Fig. 2 present the transmit and receive antenna wideband azimuthal radiation patterns (3 - 6 GHz) for an isolated case and also mounted upon the area of the body used for the specific tests, highlighting the effort of using the antenna as a body-centric wearable has on its performance. The spectral response from 3 GHz to 6 GHz for transmit and receive antennas is presented in Fig. 3 and Fig. 4 respectively with values annotated for 3, 4, 5, and 6 GHz. They depict the S_{11} values across the operating range as well as the effects of mounting the antenna onto various body positions.

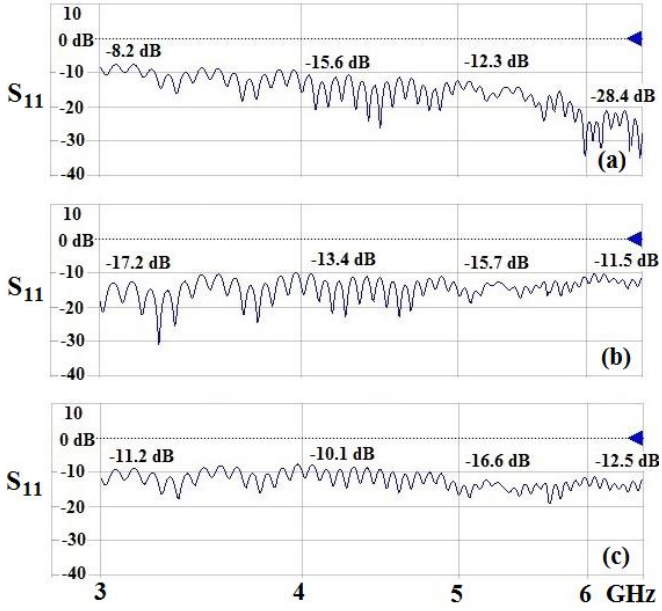

Fig. 3. Transmit antenna spectral response (S_{11}) for 3-6 GHz.
(a) Isolated antenna (b) Waist-worn antenna (c) Handheld device

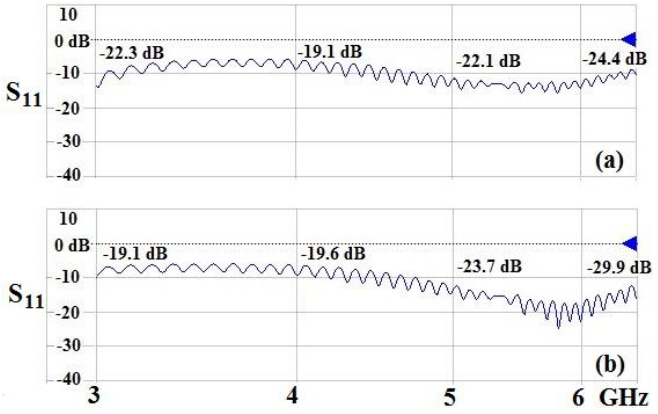

Fig. 4. Receive antenna spectral response (S_{11}) for 3-6 GHz.
(a) Isolated antenna (b) Chest-mounted antenna

A fast-processing laptop recorded the incoming channel impulse response (CIR) data at a rate of 100 samples per second which meets the Nyquist criterion for a 6 GHz node moving at 0.5 ms^{-1} (the Doppler frequency for such a mobile transmitter is 10 Hz). Each scan was post-processed by de-convolving the received CIR from a reference measurement made at 3.2m Tx-Rx separation in the anechoic chamber using a frequency domain technique to leave only the impulse response transfer function of the radio channel [24], and then transformed into a power delay profile (PDP).

All measurements were made in the time domain which has the advantage over frequency domain measurements [25] in that dynamic measurements for a moving radio can be made. The operational bandwidth of the FCC compliant UWB radio system was between 3.1 – 6 GHz with center frequency of 4.7 GHz and a launch power of –12 dBm. As the signal received can vary considerably at various locations within the environment [26] and causes data rate-limiting inter-symbol interference [27], we thus consider three parameters that suitably allow a statistical analysis of the IoT UWB hospital channel; received power levels (RSSI), mean excess delay (t_{mean}) and RMS delay spread (t_{RMS}) [28]. Mean excess delay is the first central moment of the power delay profile (PDP) which is derived from the CIR [29], expressed as:

$$t_{mean} = \frac{\sum_{i=0}^{\infty} t_i P(t_i)}{\sum_{i=0}^{\infty} P(t_i)} \quad (1)$$

The RMS delay spread is the square root of the second central element of the PDP which presents a measure of PDP temporal spread about the mean excess delay.

$$t_{RMS} = \sqrt{\frac{\sum_{i=0}^{\infty} (t_i - t_{mean})^2 P(t_i)}{\sum_{i=0}^{\infty} P(t_i)}} \quad (2)$$

B. Measurement Environment and Procedure

The measurement environment was a 61 m^2 hospital ward (Fig. 5) with 6 medical beds, privacy curtains, medication preparation area, etc. and had double-glazed PVC-framed windows along one length. The building, of late 1990's construction, was steel framed with double medium density concrete-block cavity external walls, single brick internal walls and concrete floors. A suspended ceiling supported luminaries at 2.6 m above floor level.

The patient subject was an adult male of mass 83 kg, height 1.78 m. The clinician was an adult male of mass 70 kg and height 1.70 m. The roaming clinician carried the UWB IoT radio transmitter in 2 specific locations; firstly in a handheld portable tablet-style device used for capturing notes to the Electronic Health Record (EHR) in the cubital fossa (internal elbow bend), and secondly on the belt area such as is standard practice for pagers and a popular position for medical-use smartphones. The receiver was positioned on the patient's sternum and secured using elasticated strap to eliminate antenna-body separation [30]. Two patient postures were determined to consider the 2 main bed positions; sitting up in bed and lying down in the bed. Such a change in position changes the antenna orientation as well as the physical geometry of the human body to which the IoT radio is attached. The patient lay/sat in the bed during testing while the clinician walked around the hospital ward as if on routine medical rounds (clockwise from the bottom left-hand bed) at a walking speed of 0.5 ms^{-1}.

III. Results and Discussion

The mean values attained for received power, mean excess delay (t_{mean}) and RMS delay spread (t_{RMS}) are presented in Table I for each of the specified arrangements. Results indicate that the best RSSI values, the lowest t_{mean} and smallest t_{RMS} values are seen for a waist-mounted clinician node and a reclining patient. LOS average over all arrangements is -68.6dBm while NLOS average over all arrangements is -71.9dBm. This is a seemingly small difference (3.3dBm in average power) although minimum received values for LOS and NLOS show a greater difference indicating a greater chance of deep fades in signal; this was particularly evident in waist-worn scenarios.

To best understand the distribution of the received power, t_{mean} and t_{RMS} in an IoT-enabled hospital ward we can present the results as cumulative density functions (CDF) and furthermore mathematically model the distributions to allow comparison with other results as well as produce a generic mathematical model for similar hospital wards.

A. Cumulative Density Functions (CDF)

The results were transformed into a CDF using bins assigned according to the Freedman-Diaconis rule and for each scenario the maximum likelihood (ML) estimates of each UWB parameter were calculated for popular statistical distributions and the Akaike information criterion (AIC) used to select the closest fitting distribution, as per [31].

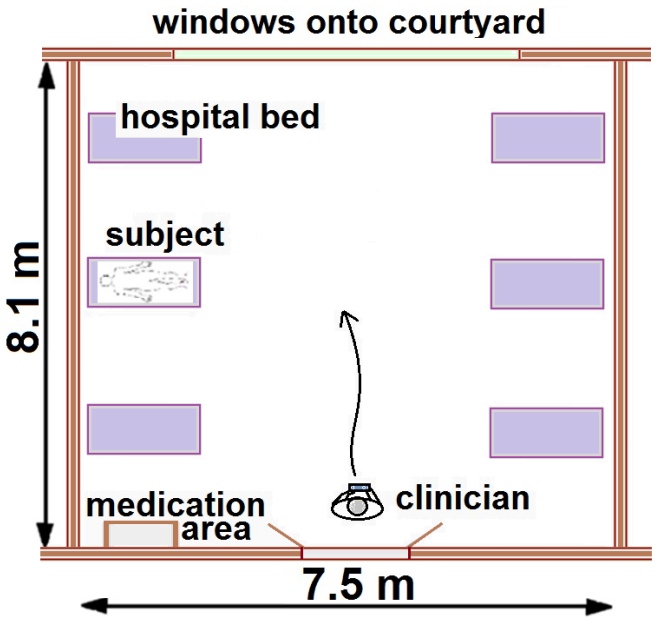

Fig. 5. Internet of Things hospital ward layout

TABLE I
STATISTICAL DISTRIBUTIONS AND PARAMETERS OF RSSI, T_{MEAN}, AND T_{RMS} FOR THE VARIOUS CONFIGURATIONS

				Statistical Parameters			
	Configuration	**Mean**	**Distribution**	**Est.**	**Std. Err.**	**Est.**	**Std. Err.**
Received power	**Waistworn-Lying**	**-68.41 dBm**	**Lognormal**	μ = 3.05	μ = 0.01	σ = 0.18	σ = 0.01
	Waistworn-Sitting	**-70.49 dBm**	**Lognormal**	μ = 2.89	μ = 0.02	σ = 0.33	σ = 0.02
	Handheld-Lying	**-71.09 dBm**	**Lognormal**	μ = 2.91	μ = 0.02	σ = 0.23	σ = 0.014
	Handheld-Sitting	**-70.35 dBm**	**Lognormal**	μ = 2.93	μ = 0.03	σ = 0.29	σ = 0.016
Mean delay	**Waistworn-Lying**	**26.16 ns**	**Weibull**	a=2.66e-08	a=6.85e-11	b= 32.85	b=2.04
	Waistworn-Sitting	**26.72 ns**	**Weibull**	a=2.72e-08	a=7.32e-11	b=32.46	b=2.12
	Handheld-Lying	**26.84 ns**	**Weibull**	a=2.75e-08	a=1.16e-10	b=22.51	b= 1.53
	Handheld-Sitting	**27.11 ns**	**Weibull**	a=2.77e-08	a=9.09e-11	b= 26.46	b= 1.84
RMS delay	**Waistworn-Lying**	**28.89 ns**	**Weibull**	a=2.93e-08	a=7.22e-11	b=34.58	b=2.06
	Waistworn-Sitting	**29.58 ns**	**Weibull**	a=2.99e-08	a=6.75e-11	b=39.06	b=2.48
	Handheld-Lying	**29.41 ns**	**Weibull**	a=3.01e-08	a=1.14e-10	b= 25.11	b=1.68
	Handheld-Sitting	**29.78 ns**	**Weibull**	a=3.04e-08	a=8.59e-11	b= 30.81	b= 2.09

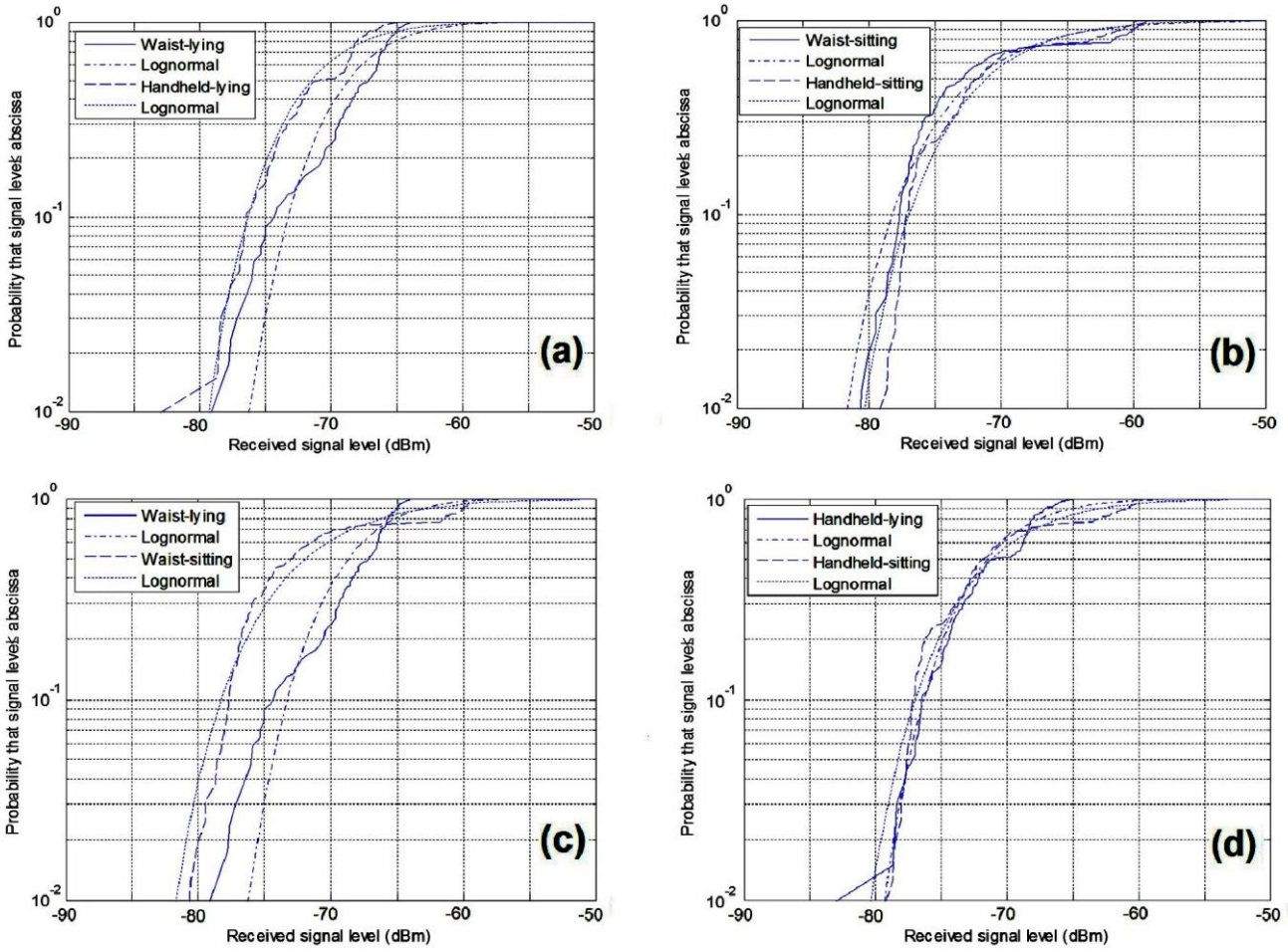

Fig. 6. CDF for RSSI. (a). Waist-mounted vs. handheld clinician node for a reclining patient, (b). Waist-mounted vs. handheld clinician node for a seated patient, (c). Patient lying vs. patient sitting for a waist-mounted clinician node, (d). Patient lying vs. patient sitting for a handheld clinician node

1) RSSI

It is inappropriate to calculate system performance by averaging the fading data due to path loss [32], for this reason a moving average window is required to remove the path loss effects (de-mean the signal). Received power values suffer from fast fading and slow fading and demeaning eliminates the local mean to prevent the local statistics from affecting the correlation of high frequency variations as the local mean contributes to the slow fading variations. The window size used for averaging should be between 2 - 64 wavelengths. For these experiments the window size used was 7.5 λ at the center frequency, which translates into a window size of 100 data points for the 1000 scans; this confirms to the recommendations stipulated by [33]. The demeaned RSSI values are presented in Fig. 6 as CDFs and are arranged to effectively compare the waist-mounted clinician node with the handheld clinician node when the patient is lying down (Fig. 6(a)); waist-mounted clinician node with the handheld clinician node when the patient is sitting up (Fig. 6(b)); the patient lying down with the patient sitting up for a waist-mounted clinician node (Fig. 6(c)); and the patient lying down with the patient sitting up for a handheld clinician node (Fig. 6(d)).

Fig. 6(a) shows that the waist-mounted clinician node had a higher RSSI than handheld clinician node for a reclining patient, while Fig. 6(b) reveals for the seated posture the waist-mounted clinician node had a similar CDF profile to a handheld clinician node, with slightly more favorable handheld RSSI levels at the lower end of the received power values. Fig. 6(c) outlines that the patient lying down had a higher RSSI than the patient sitting up for a waist-mounted clinician node, and Fig. 6(d) presents the patient lying down as having a similar CDF profile to that of the patient sitting up for a handheld node, again with slightly more favorable sitting RSSI levels at the lower end of the received power values.

Overall, there appears to be no significant RSSI penalty for changing from a handheld device to a waist-worn equivalent, with waist-worn slightly more favorable when the patient is lying down and handheld more favorable when sitting up. Handheld and sitting seem to offer the best RSSI values, however, such as the nature of UWB signals that due to the potential for multipath propagation in such an environment as a hospital ward there is a strong chance that a useable signal strength will be attained in any of the scenarios making it a good choice of IoT solution in such settings [34]. This gives a level of confidence that such an UWB IoT link would be generally robust for patients in varying postures, as well as nodes positioned either on the clinician or realized in handheld formats.

Each of the RSSI scenarios were best modelled by a lognormal distribution which reflects results from [35] which presented RSSI results from and ambulatory patient with an UWB link to a fixed wall-mounted base station, [36]

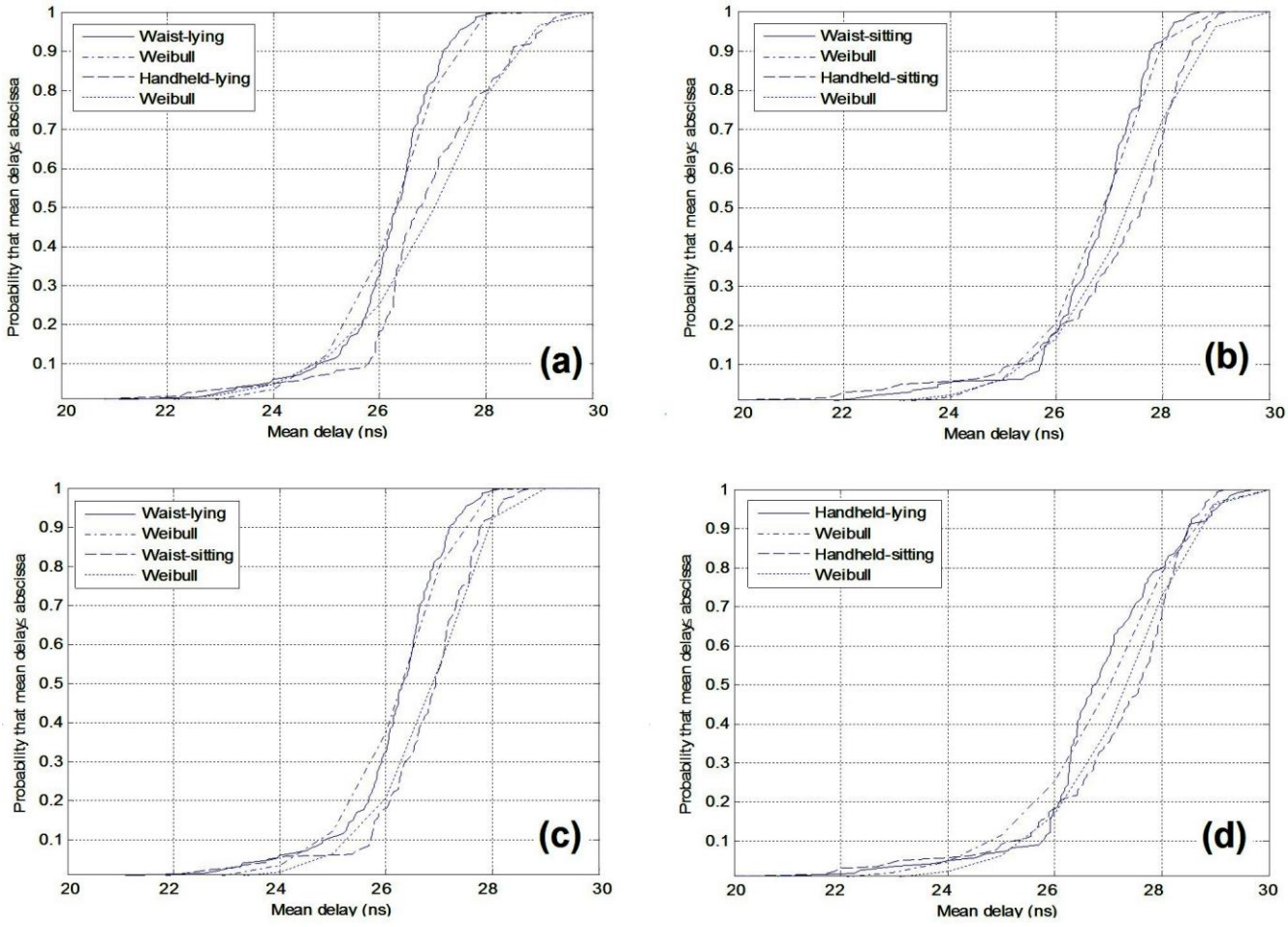

Fig. 7. CDF for Mean Excess Delay (t_{mean}). (a). Waist-mounted vs. handheld clinician node for a reclining patient, (b). Waist-mounted vs. handheld clinician node for a seated patient, (c). Patient lying vs. patient sitting for a waist-mounted clinician node, (d). Patient lying vs. patient sitting for a handheld clinician node

who investigated UWB off-body links in open apartment environments, [37] studying path loss from UWB worn radios to ceiling-mounted gateways in a lab, and [38] who measured UWB off-body links in a large classroom.

2) Mean Excess Delay (t_{mean})

The CDFs for t_{mean} are presented in Fig. 7(a-d) with comparisons as per the figure caption. Study of the CDF profiles for t_{mean} values reveal that the waist-worn clinician radio exhibits less mean delay than the handheld equivalent for a reclining patient (Fig. 7(a)), while Fig. 7(b) shows the waist-worn radio exhibits less mean delay than the handheld radio for a patient in the seated position. Furthermore Fig. 7(c) depicts a reclining patient scenario as having less mean signal delay compared to a sitting patient for a waist-mounted clinician node, and the same is seen for the reclining versus sitting arrangement for the clinician carrying a handheld device (Fig. 7(d)). In each test the difference in mean delay are generally small which highlights the general lack of reliance on the patient or clinician being in a required position to ensure quality IoT data transfer and suggests that such a system would duly offer predictable operation in a hospital ward over the full medical round visitation. When mean delay results were split into respective LOS and NLOS divisions the NLOS has greater t_{mean} values than the LOS which is to be expected due to the geometry; however the difference is not particularly large at between 10-13ns for the various permutations of transmitter and receiver location. This is a strong recommendation for the use of UWB as an enabling IoT technology in such environments as it is robust to body shadowing which would happen regularly as the clinician and patients move. Each of the mean excess delay scenarios were best modelled by a Weibull distribution which reflects results from [35] which studied a hospital with a roaming UWB node but a fixed wall-mounted base station.

3) RMS Delay Spread (t_{RMS})

Study of the CDF profiles for t_{RMS} values reveal a similar pattern to CDF profiles for t_{mean} values with the waist-worn clinician radio exhibiting less RMS delay spread than the handheld equivalent for a reclining patient (Fig. 8(a)), the waist-worn radio exhibiting RMS delay spread than the handheld radio for a patient in the seated position (Fig. 8(b)), the reclining patient scenario as having less RMS delay spread compared to a sitting patient for a waist-mounted clinician node (Fig. 8(c)), and the reclining patient scenario as having less RMS delay spread compared to a sitting patient for a clinician carrying a handheld device (Fig. 8(d)). As for mean delay, the RMS delay spread differences are generally small which reaffirms the supposition of such an UWB IoT system offering robust operation in a hospital ward. Moreover, these values are in

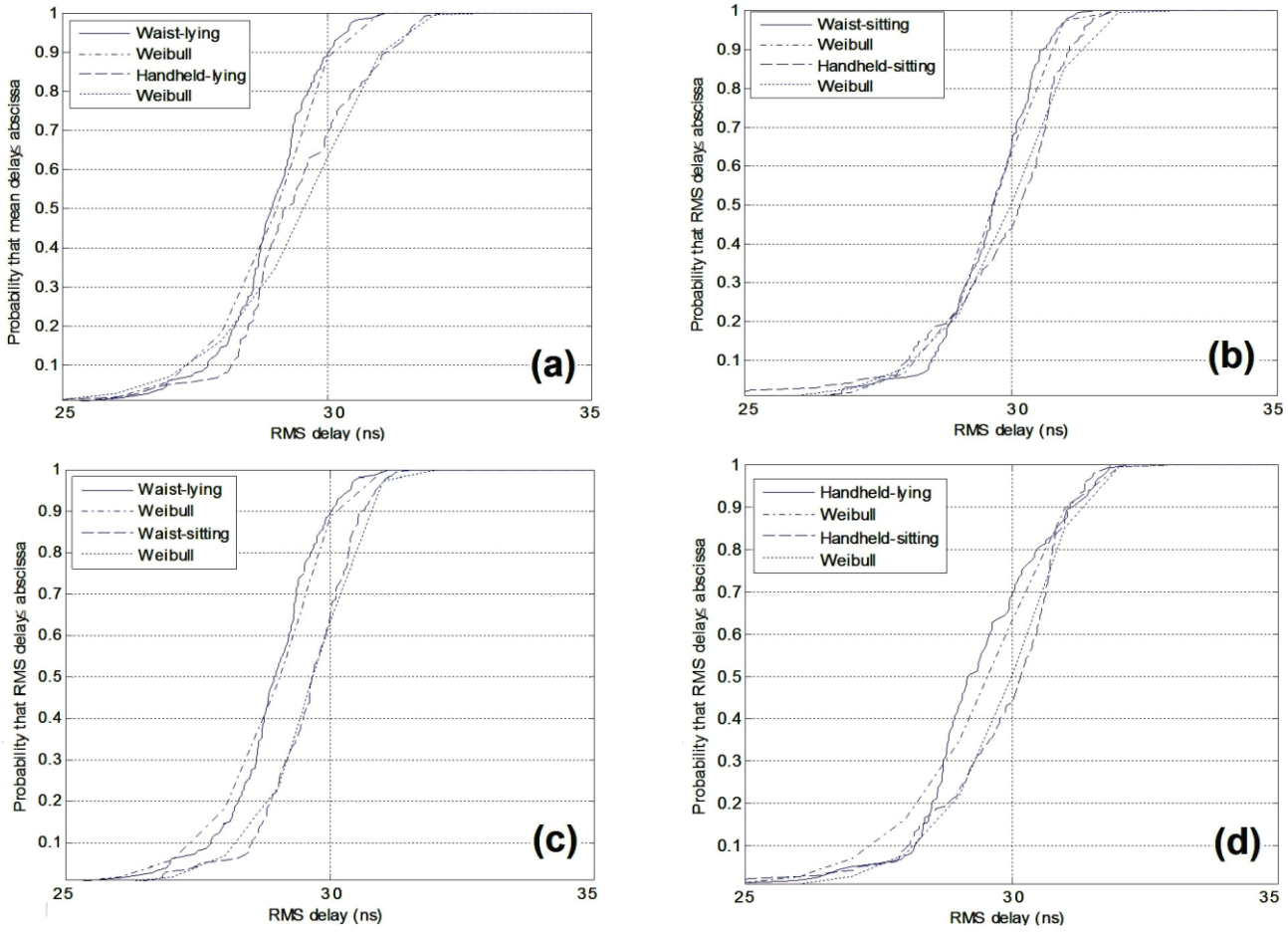

Fig. 8. CDF for RMS Delay Spread (t_{RMS}). (a). Waist-mounted vs. handheld clinician node for a reclining patient, (b). Waist-mounted vs. handheld clinician node for a seated patient, (c). Patient lying vs. patient sitting for a waist-mounted clinician node, (d). Patient lying vs. patient sitting for a handheld clinician node

keeping with RMS delay spread values for similarly sized environments with fixed base stations revealing that the body-to-body aspect of such an IoT medical link arrangement makes no greater impact on the likelihood of inter-symbol interference (ISI) which is recognized as having a detrimental effect on maximum achievable data rates [39]. Each of the t_{RMS} CDFs were best modelled by a Weibull distribution, as per [35].

B. Further Observations

In the hospital environment there was additional fading observed when the clinician's body is blocking the signal (NLOS) compared with a direct ray condition (LOS). This was determined to be an additional loss of 7.6 dB for handheld and 6.9 dB for waist worn when the patient was sitting, and 7.1 dB for handheld and 6.6 dB for waist worn with the patient reclined. The additional body shadowing losses were less for the reclined compared to the sitting position. The time dispersal measurements supported this with an average increase in mean delay of 3.5ns and 2.1ns in RMS delay spread for NLOS compared to LOS scenarios.

With regards to the small scale fading it was observed that regular rapid RSSI fluctuations in the region of 5dB occurred as the clinician moved around the ward. The depths of the small scale fades did not depend notably on whether the transmitter was handheld of waist worn or whether the patient was seated or reclined.

The channel gain of the system was affected with the Tx-Rx antenna orientations. Additional testing (conducted in the environment at 3 m patient-clinician separation) confirmed that when both antennas were effectively side facing compared with face-on there was an additional loss of 10.2 dB for handheld and 8.4 dB for waist worn when the patient was sitting and 9.9 dB for handheld and 9.3 dB for waist worn with the patient reclined.

IV. CONCLUSIONS

This paper presented empirical measurement results from a campaign to characterize and mathematically model the radio channel for a medical UWB Internet of Things link for a patient and a roaming clinician within a contemporary hospital. Patient orientation effects on the received signal strength, mean excess delay, and RMS delay spread values were investigated for a clinician conducting routine ward rounds. The results of each recommend the use of UWB as an enabling IoT technology in hospital environments with bodyworn systems and would be generally robust for patients in varying postures, as well as nodes positioned upon the clinician or embedded into handheld formats. The authors believe this work to be a valuable contribution to understanding how the Internet of Things technology of UWB will perform in the hospitals of the future for wearable smart devices and expect this publication to generate considerable interest and discussion.

REFERENCES

[1] P.A. Catherwood, W.G. Scanlon, "Ultrawideband Communications—An Idea Whose Time has Still Yet to Come?", *IEEE Ant. and Prop. Mag.*, vol.57, no.2 pp.38-43, 2015.

[2] B. Lewis, "UWB is back … this time for IoT location-based services", *Embedded Comp. Design*, vol.12, no.7, pp.8, Nov. 2014.

[3] M. Charlier, B. Quoitin, S. Bette, J. Eliasson, "Support for IEEE 802.15.4 ultra wideband communications in the Contiki operating system," *2016 Symp. on Comms. and Veh. Tech.*, 2016, pp. 1-6.

[4] A. Bekasiewicz, S. Koziel, "Compact UWB monopole antenna for internet of things applications", *Electronics Letters*, vol.52, iss.7, pp.492-494, April 2016.

[5] M. Hernandez-Silveira, K. Wieczorkowski-Rettinger, S. Ang, A. Burdett, "Preliminary assessment of the SensiumVitals: A low-cost wireless solution for patient surveillance in the general wards", *Ann. Intl. Conf. IEEE Eng. Med. Biol. Soc.*, Milan, 2015, pp. 4931-4937.

[6] C.E. Tung, D. Su, M.P. Turakhia, M.G. Lansberg, "Diagnostic Yield of Extended Cardiac Patch Monitoring in Patients with Stroke or TIA", *Frontiers in Neurology*, vol.5, pp.266, Jan 2015.

[7] C. Imison, S. Castle-Clarke, R. Watson, N. Edwards, "Delivering the benefits of digital health care", *Nuffield Trust*, pp. 5, 2016.

[8] J. Dunhill, "NHS England: Digital plans could save £10bn", *Health Service Journal*, June 2015.

[9] Gartner, Inc. Online: http://www.gartner.com/newsroom/id/2905717 (Accessed 27/06/16).

[10] United Nations, Department of Economic and Social Affairs, "World Population Ageing 2013". ST/ESA/SER.A/348.

[11] N.N. Dhalwani et al., "Long terms trends of multimorbidity and association with physical activity in older English population", *Intl. J. Beh. Nutrition and Physical Act.*, vol.13, no.8, 2016.

[12] J. Henriques et al., "Prediction of Heart Failure Decompensation Events by Trend Analysis of Telemonitoring Data", *IEEE J. Biomed. and Health Informatics*, vol.19, no.5, pp.1757-1769, Sept. 2015.

[13] A. Appari, E.K. Carian, M.E. Johnson, D.L. Anthony, "Medication administration quality and health information technology: a national study of US hospitals", *J. of the American Medical Informatics Association*, vol.19, no.3, pp. 360-367, 2012.

[14] J.R. Stachel, E. Sejdic, A. Ogirala, M.H. Mickle, "The impact of the internet of Things on implanted medical devices including pacemakers, and ICDs," *Instr. and Meas. Tech. Conf. (I2MTC), IEEE Intl.*, pp.839-844, 6-9 May 2013.

[15] J.R. Stachel, E. Sejdic, A. Ogirala, M.H. Mickle, "The impact of the internet of Things on implanted medical devices including pacemakers, and ICDs," *Instr. and Meas. Tech. Conf. (I2MTC), IEEE Intl.*, 6-9 May 2013, pp.839-844.

[16] T. Kumpuniemi, M. Hämäläinen, K.Y. Yazdandoost, J. Iinatti, "Measurements for body-to-body UWB WBAN radio channels," *2015 9th Euro. Conf. Ant. and Prop. (EuCAP)*, Lisbon, 2015, pp.1-5.

[17] Y. Wang, I.B. Bonev, J.Ø. Nielsen, I.Z. Kovacs, G.F. Pedersen, "Characterization of the Indoor Multi-antenna Body-to-Body Radio Channel," *IEEE Trans. on Ant. and Prop.*, vol.57, no.4, pp.972-979, April 2009.

[18] E. Ben Hamida, M. M. Alam, M. Maman, B. Denis, R. D'Errico, "Wearable Body-to-Body networks for critical and rescue operations - The CROW^2 project," *IEEE 25th Ann. Intl. Symp. Per., In., Mob. Radio Comm. (PIMRC)*, Washington DC, 2014, pp. 2145-2149.

[19] R. Rosini, R. Verdone, R. D'Errico, "Body-to-Body Indoor Channel Modeling at 2.45 GHz," *Antennas and Propagation, IEEE Transactions on*, vol.62, no.11, pp.5807-5819, Nov. 2014.

[20] E. Vinogradov, W. Joseph, C. Oestges, "Measurement-Based Modeling of Time-Variant Fading Statistics in Indoor Peer-to-Peer Scenarios," *IEEE Trans. on Ant. and Prop.*, vol.63, no.5, pp.2252-2263, May 2015.

[21] H.G. Schantz, "Bottom fed planar elliptical UWB antennas," *IEEE Conf. on Ultra Wideband Sys. and Tech.*, 2003, pp. 219-223.

[22] H. Schantz, "Planar Elliptical Element Ultra-Wideband Dipole Antennas," *IEEE APS*, 2002.

[23] H. Schantz, "Apparatus for establishing signal coupling between a signal line and an antenna structure" U.S. Pat. 6,512,488 (28/1/03).

[24] System Analysis Module User's Manual PulsON210 UWB Reference Design, (Document P210-320-0102B), Aug. 2005.

[25] B. Hanssens *et al.*, "An indoor localization technique based on ultra-wideband AoD/AoA/ToA estimation," *2016 IEEE Intl. Symposium on Ant. and Prop.*, Fajardo, 2016, pp. 1445-1446.

[26] R.J.C. Bultitude, R.F. Hahn, R.J. Davies, "Propagation considerations for the design of an indoor broad-band communications system at EHF", *IEEE Trans. Veh. Tech.*, vol.47, no.1, pp.235-245, Feb. 1998.

[27] T.S. Rappaport, "Wireless Communications: Principles & Practice," 2nd Ed., Prentice-Hall, NJ, 2002,

[28] C.M.P. Ho, et al, "Antenna Effects on Indoor Obstructed Wireless Channels and a Deterministic Image-Based Wide-Band Propagation Model for In-Building Personal Communication Systems", *Intl. J. Wireless Info. Networks*, pp. 61-76, 1994.

[29] J.B. Andersen, T.S. Rappaport, S. Yoshida, "Propagation measurements and models for wireless communications channels", *IEEE Comms. Mag.*, vol.33, no.1, pp.42–49. Jan. 1995.

[30] P.A. Catherwood, W.G. Scanlon, "Measurement Errors Introduced by the Use of Co-axial Cabling in the Assessment of Wearable Antenna Performance in Off-body Channels", *European Conf. Ant. and Prop. 2011 (EuCAP)*, Rome, pp.3787-3791, 11-15 April 2011.

[31] K.P. Burnham, D.R. Anderson, "Model Selection and Multimodel Inference", Springer, USA, 2002.

[32] R.H. Clarke, "Statistical Theory of Mobile-Radio Reception," *Bell System Tech. J.*, vol.47, pp.957-1000, July 1968.

[33] J.D. Parsons, M.F. Ibrahim, "Signal strength prediction in built-up areas. Part 2: Signal variability," *IEE Proc. Comms., Radar and Signal Proc.*, vol.130, no.5, pp.385-391, Aug. 1983.

[34] R. Zetik, M. Eschrich, S. Jovanoska and R. S. Thoma, "Looking behind a corner using multipath-exploiting UWB radar," in *IEEE Trans. Aero. Electr. Sys.*, vol.51, no.3, pp.1916-1926, July 2015.

[35] P.A. Catherwood, W.G. Scanlon, "Off-body UWB channel characterisation within a hospital ward environment," *International. J. Ultra Wideband Comm. & Systems*, vol.1, no.4, pp.263-272, 2010.

[36] C. Chong, K. Youngeil, L. Seong-Soo, "A statistical based UWB multipath channel model for the indoor environments", *IEEE Intel. Vehicles Symp. WPAN Applications*, 6–8 June 2005, pp.525–530.

[37] M. M. Khan, Q. H. Abbasi, A. Alomainy, Y. Hao, C. Parini, "Experimental characterisation of ultra-wideband off-body radio channels considering antenna effects," in *IET Microwaves, Antennas & Propagation*, vol.7, no.5, pp.370-380, April 11 2013.

[38] P.A. Catherwood, W.G. Scanlon, "Body-centric antenna positioning effects for off-body UWB Communications in a contemporary learning environment," *Proc. of the 8th Euro. Conf. Ant. and Prop. (EuCAP)*, Rome, pp.3787-3791, 11-15 April 2011.

[39] A. Ramesha, A. Nareshb, N.V. Seshagiri Raoc, "Technique for Reduction of Intersymbol Interference in Ultra- Wideband System", *Intl. Conf. Em. Trends Eng., Sci. & Tech.*, vol.24, 2016, pp.812–819.